

# The radio luminosity distribution of pulsars in 47 Tucanae

D. McConnell<sup>1</sup>, A.A. Deshpande<sup>1,2,3</sup>, T. Connors<sup>4,5</sup> & J.G. Ables<sup>6</sup>

<sup>1</sup> Australia Telescope National Facility, CSIRO, PO Box 76, Epping, NSW 1710, Australia

<sup>2</sup> Raman Research Institute, Bangalore 560 080, India

<sup>3</sup> Present address: Arecibo Observatory, NAIC, HC3 Box 53995, Arecibo, Puerto Rico

<sup>4</sup> Department of Physics, University of Sydney, Australia

<sup>5</sup> Present address: Centre for Astrophysics and Supercomputing, Swinburne University, PO Box 218, Hawthorn, Vic 3122, Australia

<sup>6</sup> Telecommunications and Industrial Physics, CSIRO, PO Box 76, Epping, NSW 1710, Australia

10 April 2018

## ABSTRACT

We have used the Australia Telescope Compact Array to seek the integrated radio flux from all the pulsars in the core of the globular cluster 47 Tucanae. We have detected an extended region of radio emission and have calibrated its flux against the flux distribution of the known pulsars in the cluster. We find the total 20-cm radio flux from the cluster’s pulsars to be  $S = 2.0 \pm 0.3$  mJy. This implies the lower limit to the radio luminosity distribution to be  ${}^{\min} L_{1400} = 0.4$  mJy kpc<sup>2</sup> and the size of the observable pulsar population to be  $N \lesssim 30$ .

## 1 INTRODUCTION

Pulsars fall into two quite distinct categories: young objects with relatively low spin rate — standard pulsars; and much older objects spinning several hundred times per second — the so-called millisecond pulsars. The majority of known pulsars fall into the former category and are distributed across the Galactic disk as expected for objects that have originated fairly recently ( $10^4 - 10^7$  years) from massive stellar supernovae. The millisecond pulsars have quite a different distribution, but which can also be understood by looking at their progenitors. Srinivasan & van den Heuvel (1982) and Alpar et al. (1982) proposed that the millisecond pulsars have been spun up to high rotation rates during an accretion phase as a member of low mass X-ray binary (LMXB) systems. The tendency for millisecond pulsars to be found in globular clusters is seen as a natural consequence of the high incidence of LMXB systems in such clusters. Of the galactic globular clusters, 47 Tucanae dominates as the host of at least 22 pulsars (Manchester, 2000). This number is large enough that it presents the possibility of certain population studies, some of which have been addressed by Camilo et al. (2000) and Friere et al. (2001).

In this paper we discuss the number of potentially observable pulsars in 47 Tucanae. We use the term “potentially observable” (sometimes simply “observable”) for pulsars whose emission beam passes over the Earth and so could be detected with a sufficiently sensitive telescope. The probability that any pulsar is potentially observable depends on the angular width of its emission beam, and the fraction of all pulsars that are observable relates to some population average (latitudinal) beam width.

Camilo et al. have estimated the total number of potentially observable pulsars in 47 Tuc to be  $\sim 200$ . They base their estimate on the supposition that the cluster pulsars are

distributed in luminosity according to the law observed for the standard pulsars in the Galactic disk. That is, their differential luminosity distribution is assumed to be consistent with

$$d \log N = -d \log L \quad (1)$$

where  $N$  is the number of pulsars and  $L$  their luminosity. Camilo et al. also assumed that the pulsars extend in luminosity down to the lower limit observed in the Galactic pulsar population, measured at 400 MHz, of  ${}^{\min} L_{400} \sim 1$  mJy kpc<sup>2</sup>.

The determination of the luminosity distribution for a population of pulsars is a difficult process (see for example Lyne, Manchester & Taylor, 1985) for the following reasons. Firstly, the distance to each pulsar in the sample must be known. This is usually inferred from the observed dispersion of the pulsar signal and estimates of the free electron density along the interstellar line of sight and is often given with large uncertainty. Secondly, any sample is incomplete because of observational selection effects. This is particularly relevant for the fainter pulsars in the population and introduces extra uncertainty in the measured luminosity function at the low-luminosity end of the distribution.

A measurement of the total radio flux from the core region of 47 Tucanae would, if the form of the pulsar flux distribution were known, provide an estimate of the lower limit to the distribution and of the number of pulsars in the cluster. Specifically, if the cluster contains the estimated 200 observable pulsars and if the flux distribution as assumed by Camilo et al. is followed, the total radio flux from the pulsars in the cluster core should be  $\sim 4$  mJy — double that of those already detected. Here we report observations designed to be sensitive to such a distribution of 20 cm emission from the core. The observations reported here were made with the Australia Telescope Compact Array (ATCA) in low resolu-

tion (short baseline) configurations and are complementary to earlier higher resolution ATCA observations reported by McConnell & Ables, 2000 (referred to hereafter as MA2000) and McConnell, Deacon & Ables, 2001 (MDA2001).

## 2 THE PULSAR LUMINOSITY DISTRIBUTION

The observed radio luminosity of a pulsar is

$$L = sD^2 \quad (2)$$

where  $s$  is its radio flux and  $D$  its distance from the observer.  $L$  is usually expressed in the units mJy kpc<sup>2</sup>. The distance to 47 Tuc is  $4.5 \pm 0.3$  kpc (Zoccali et al., 2001). In equation (2), the distance  $D$  to all pulsars in 47 Tuc is effectively the same. Given the angular spread on the sky of the 47 Tuc pulsars  $\Delta\theta \leq 2.5$ , and assuming the distribution to be symmetrical, the spread in pulsar distance  $\Delta D \leq D\Delta\theta \simeq 3$  pc is negligible. In the following we describe the distribution of radio fluxes, and in conclusion give the equivalent parameters of the luminosity distribution for comparison with the general pulsar population.

As noted in the introduction, the population of standard pulsars in the Galactic disc has a luminosity distribution consistent with equation 1. It is useful to write explicitly the underlying frequency distribution and to determine whether the 47 Tuc pulsars with known fluxes also belong to a population consistent with that relation. We write the frequency distribution of pulsars,  $n(s)$ , with radio flux  $s$  as

$$n(s)ds = \begin{cases} 2Ns_{min}s^{-2}ds & s \geq s_{min} \\ 0 & s < s_{min} \end{cases} \quad (3)$$

where

$$\int_{s_{min}}^{\infty} n(s)ds = N \quad (4)$$

is the total size of the pulsar population. The cumulative frequency distribution  $N(> s)$ , ie. the number of pulsars with flux density greater than  $s$ , is then

$$N(> s) = \int_s^{\infty} n(x)dx = \frac{Ns_{min}}{s} \quad (5)$$

for  $s > s_{min}$ . After taking the logarithm we get

$$\log N(> s) = \log Ns_{min} - \log s \quad (6)$$

which, in differential form, corresponds to equation 1. For such a distribution, the integrated flux of all pulsars with flux above some limit  $s$  is

$$S(> s) = Ns_{min} \sum_{k=1}^m \frac{1}{k} \quad (7)$$

where  $m = Ns_{min}/s$ .

To verify that equation 6 describes the sample of pulsars already detected in 47 Tuc, we have analysed their fluxes reported by Camilo et al. (2000). We give their cumulative flux distribution  $N(> s)$  in Figure 1, which shows that pulsars with  $s \gtrsim 0.07$  mJy follow the assumed law. Fainter pulsars appear to be less numerous, as might be expected either because of approaching the sensitivity limit of the detection equipment or because the intrinsic lower flux limit is

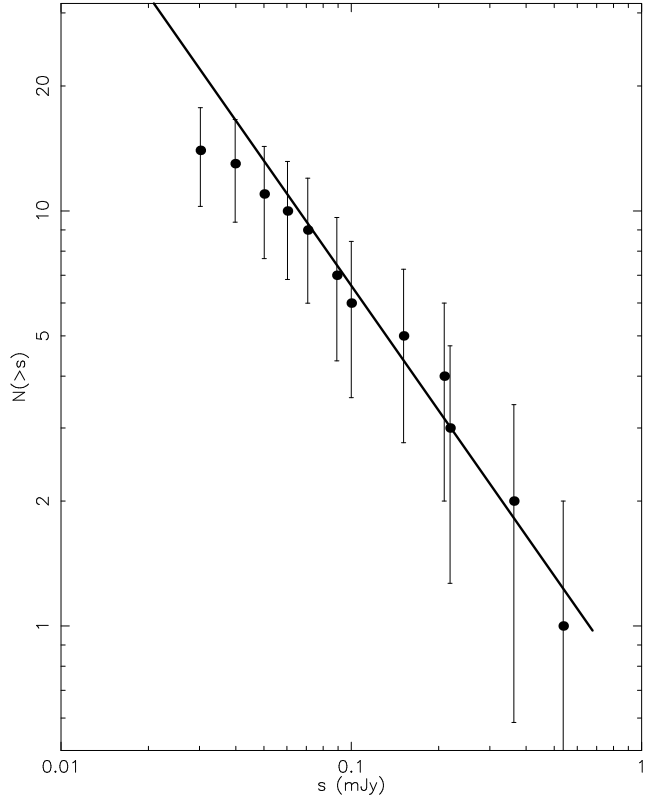


**Figure 1.** The cumulative distribution of 47 Tuc pulsars with respect to 20 cm radio flux taken from Camilo et al. (2000). The line is a fit to the distribution for pulsars with  $s \geq 0.07$  mJy, constrained to have slope  $b = -1$ :  $\log N(> s) = -0.18 - \log s$ .

being approached. We have fitted the cumulative distribution for  $s \geq 0.07$  mJy (9 pulsars) to an expression of the form  $\log N(> s) = a + b \log s$  and find that  $a = -0.1 \pm 0.2$ ,  $b = -0.9 \pm 0.2$ , consistent with equation 6. Constraining the distribution to follow equation 6 exactly ( $b = -1$ ) we find

$$\log N(> s) = -0.18 \pm 0.07 - \log s \quad (8)$$

This indicates that the quantity  $Ns_{min} \simeq 0.66 \pm 0.11$  mJy.

## 3 OBSERVATIONS AND DATA ANALYSIS

The aim of the observations reported here was to detect radio emission from the core of 47 Tucanae. The likely distribution of pulsars in the cluster has already been indicated by the positions of the brighter members as determined from pulse timing analysis (Freire et al., 2001). We sought to detect the integrated emission of a possibly larger population of pulsars sharing this spatial distribution. All pulsars lie within  $3.2 r_c$  of the cluster centre, where the core radius  $r_c = 23.1'' \pm 1.7''$  (Howell, Guhathakurta & Gilliland, 2000). We therefore chose to use the Australia Telescope Compact Array in the 0.75 and 0.375 configurations to give sensitivity to brightness distributions of order  $\sim 50''$  in size. The observations were made over a bandwidth of 128 MHz centred at 1.408 GHz ( $\lambda \sim 20$  cm).

The MIRIAD data reduction package was used to calibrate the data and form images. The antenna gains were

**Table 1.** Summary of the ATCA observations of 47 Tucanae.

Date (UT)	Time (UT)	Integration (hours)	Array
2000 Aug 05	14:16	9.0	0.375
2000 Dec 24	00:10	11.2	0.75C
2000 Dec 25	23:13	18.7	0.75C
2000 Dec 27	11:59	8.9	0.75C

calibrated using brief observations of the source B2353-696 ( $S_{1.4} = 1.05$  Jy). The flux scale was referred to the ATCA primary flux calibrator B1934-638 ( $S_{1.4} = 14.9$  Jy). Some improvement to the antenna gain calibration was achieved by self calibration of the final image.

The images we present here were derived from the observations listed in Table 1. Care was taken to image a large area ( $137' \times 137'$ ) to cover the annular region of sky falling in the first sidelobe of the 22m antenna beam pattern which lies about  $60'$  from the centre of the primary lobe. A number of sources with flux density of up to  $\sim 6$  mJy were detected in the first sidelobe.

#### 4 IMAGE ANALYSIS

The image is dominated by the many background sources in the field, the brightest having a flux of  $\sim 50$  mJy and lying  $6.5'$  from the image centre. The effect of these sources (including their possible variability), combined with unmodelled antenna gain variations, is to increase the image noise from the  $20\mu\text{Jy}/\text{beam}$  expected from thermal (receiver and sky) fluctuations to the measured value of  $\sigma = 60\mu\text{Jy}/\text{beam}$ . Nonetheless, a diffuse area of 20-cm emission is visible in the cluster core region of the image shown in Figure 2.

Before measuring the flux of that emission and attributing it to the cluster pulsars, we must consider a number of effects associated with flux calibration, the sensitivity of the array to extended emission and pulsar variability, all of which may influence the measurement we wish to make, and its interpretation.

##### 4.1 Sensitivity to extended emission

The expected spatial extent of pulsar radio emission is indicated by the radial distribution of the 15 pulsars with locations derived from pulse timing analysis (Friere et al., 2001). These pulsars, to an approximation sufficient for our purposes, are uniformly distributed in radial distance from the cluster centre out to  $3.2r_c$ . Thus half the pulsar radio flux is expected from the inner quarter of a circle of radius  $\sim 75''$ . To test the sensitivity of the ATCA to the pulsar flux we constructed a simulated visibility dataset using the same antenna locations, observation hour angles and receiver noise characteristics as those of the real observations. To these data we added contributions corresponding to: (i) a circular source with total flux 1 mJy and a gaussian profile of full width to half maximum of  $75''$ ; (ii) a set of 17 point sources whose fluxes (each  $< 100\mu\text{Jy}$ , total  $946\mu\text{Jy}$ ) were drawn from the distribution described in section 2 and

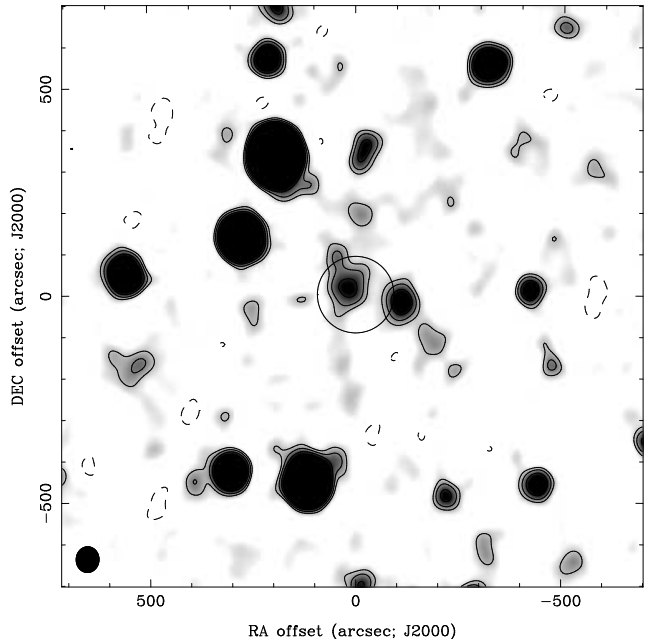


**Figure 2.** 20-cm image of 47 Tucanae. The circle is centered on the cluster centre and has radius  $4 \times r_c$  where  $r_c = 23.1''$ . The size of the restoring beam is shown at lower left. Image brightness is shown as contours at  $-3, 3, 5$  &  $8 \times$  the rms fluctuation in the image of  $\sigma = 60\mu\text{Jy}$ .

whose positions were drawn from the uniform radial distribution mentioned above. In the images derived from both these trial datasets the measured flux of the added component differed from the expected value by less than the standard error expected from the simulated thermal noise. We conclude that the baseline lengths used in the observations adequately sample the spatial scales present in the likely pulsar emission.

##### 4.2 Flux calibration

We aim to compare the radio flux of pulsars measured with the Parkes radiotelescope (Camilo et al., 2000) against the flux of radio sources in images formed with the ATCA. Therefore it is necessary to ensure consistency between the flux scales used in the two sets of measurements. In the case of the Parkes observations the pulsar time series signal strength is compared to the amplitude of noise fluctuations arising from components of the receiving equipment and from the sky — the so-called system equivalent flux density. Camilo et al. estimate a systematic uncertainty of order 25% in their published flux scale. The amplitudes of the visibilities measured with the ATCA were calibrated using observations of the source B1934-638. No specific attempt has been made to tie together the flux scales of the two instruments (F. Camilo, private communication).

To make a direct comparison we use flux measurements of the five strongest pulsars (C, D, E, F and J) with both instruments: the Parkes measurements are those of Camilo et al. (2001); the ATCA measurements are from the earlier high resolution observations (MDA2001) which, unlike the observations described here, used the 6-km configurations

of the ATCA to achieve its highest possible resolution. The measurement results appear in Table 2. We use the symbol  $S$  for integrated fluxes, distinguishing between the bright (five brightest) and faint (sixth brightest and fainter) pulsars with the leading superscripts  $b$  and  $f$ ; hence  ${}^bS_P$  is the sum of fluxes for pulsars C, D, E, F and J measured at Parkes, and  ${}^fS_A$  is the ATCA measurement of flux from all fainter pulsars. We calculate the total fluxes:

$${}^bS_P = 1.48 \pm 0.09 \text{ mJy} \quad (9)$$

$${}^fS_A = 1.20 \pm 0.16 \text{ mJy} \quad (10)$$

To validly compare fluxes measured in the ATCA images with the flux distribution quoted by Camilo et al. we scale the ATCA data by the factor  ${}^bS_P/{}^fS_A = 1.23 \pm 0.18$ . This factor is consistent with the Parkes flux scale uncertainty of  $\sim 25\%$  estimated by Camilo et al.

### 4.3 Pulsar variability

A remarkable feature of the 47 Tuc pulsars is their strong scintillation. Camilo et al. (2000) report that pulsar fluxes measured over a series of 17.5-minute observations may vary by factors of up to  $\sim 30$ . In MDA2000 we reported variability of the imaged pulsars over a series of 12-hour integrations. We have extended that analysis using the additional ATCA observations described in MDA2001 and find that the measured fluxes of an individual pulsar from a set of  $\sim 12$ -hour integrations has a standard deviation approximately equal to the mean flux of that pulsar. Note that for diffractive scintillation, the expected exponential distribution of fluxes (Rickett, 1977) has standard deviation equal to the mean, consistent with this observation. Thus, even over the 48-hour integration of Figure 1, scintillation of the brightest pulsars in the cluster could significantly influence the integrated flux from the core and take us to a misleading conclusion.

It is relevant to consider the variability of total flux of the cluster's pulsar population. Consider a set of variable sources each with mean flux  $s_i$  and rms fluctuations in flux of  $\delta s_i \sim f \times s_i$  after integration over time  $\tau$ , where  $f$  is fixed for the whole population. Then if the sources have a luminosity function as given by equation (1), it follows that the rms fluctuation of the total flux is

$$\Delta S \simeq 1.3 f s_{max} \quad (11)$$

where  $s_{max}$  is the flux of the brightest member of the set. In the case of the 47 Tuc pulsars  $f \sim 1$  for 12-hour integrations, so we would expect 12-hour measurements of the total flux to fluctuate with  $\Delta S \sim 0.7 \text{ mJy}$ . This quantity is dominated by scintillations of the brightest pulsars in the cluster. Independent measurements of their individual fluxes over the integration period considered would improve the estimate of the mean total flux, provided the measurement error is less than the expected rms fluctuation over the same period.

The image presented in Figure 1 was observed with five elements of the ATCA arranged to give baselines of up to 750m, chosen to give best brightness sensitivity to extended emission, but which naturally lacks the angular resolution to measure fluxes of individual pulsars. However, the ATCA has a sixth element fixed permanently 3km from the rail track supporting the moveable five, so that each observation

included visibility measurements from five baselines with lengths in the ranges 4.3 – 5.0 km (0.75C array) or 5.5 – 6.0 km (0.375 array). The image derived from all baselines, inspite of the poor sampling of the uv-plane, has a synthesised beam of  $4''.1 \times 3''.5$  and so is sensitive to point sources. The image has noise fluctuations of  $\sigma = 40 \mu\text{Jy}/\text{beam}$  and all of the brightest five pulsars are visible at  $> 3\sigma$  (Table 2, column 4). Thus flux measurement of the five brighter pulsars introduces significantly less uncertainty ( $\sim \sqrt{5} \times 0.04 \text{ mJy}$ ) than expected from the scintillations.

### 4.4 Image quality in the presence of variable sources

The fidelity of radio aperture synthesis images depends on the constancy of the region being imaged. In reality variable sources exist and some degradation of any 20cm image from the ATCA can be expected. For these observations we expect the pulsars themselves to vary. The diffraction responses around a variable source will differ from the point spread function of the observation and so will not be modelled correctly during deconvolution. In aperture synthesis the point spread function has zero mean, so that the effect on the image some distance from the varying source will be as often positive as negative. The effect of a number of independently varying sources in the field is to increase the background fluctuations in the image. The images presented here have rms brightness fluctuations  $\sigma = 60 \mu\text{Jy}/\text{beam}$ , compared with the value  $\sigma = 20 \mu\text{Jy}/\text{beam}$  expected from thermal considerations alone. We can attribute at least part of this extra noise to variations in the background sources.

To gauge the size of fluctuations induced by source variability we have artificially added a 0.5mJy source to the observed data over a 11-hour section of the 48-hour integration and determined the effect on the flux measured in the core of the cluster. With the artificial source placed in the core, the measured flux is increased by the expected time averaged flux of  $\sim 0.12 \text{ mJy}$ . If the test source is placed outside the core region, the influence is position dependent, but the change to the measured core flux is  $\lesssim 25 \mu\text{Jy}$ .

### 4.5 Analysis method

To determine the best possible estimate of the total pulsar flux, on a scale that allows direct comparison with the flux distribution analysed in section 2, we have analysed the data in the steps described below.

- Measure the fluxes for all pulsars above a  $3\sigma$  detection limit in the high resolution image described in section 4.3.
- Subtract from the low resolution visibility data, a set of point source responses with the measured fluxes at the corresponding pulsar locations.
- Subtract from the low resolution visibility data all source components detected in the high resolution image outside the circular region centred on the core with radius  $4r_c$ .
- Subtract an additional source (S176 in MDA2001) which lies within  $4r_c$  of the cluster centre. This source was discussed in MDA2001. It lacks variability, has a flat spectrum and is not suspected of being a pulsar.

**Table 2.** Flux measurements of the pulsars in 47 Tucanae. (2): fluxes measured at Parkes (Camilo et al., 2001). (3): fluxes measured from the ATCA image reported in MDA2001. (4): fluxes in the image formed from the long baseline data as part of the observations listed in Table 1. Uncertainties in the last digits quoted in (2),(3) appear in parentheses. The uncertainties of values in (4) are  $\sim 0.04$  mJy.

Pulsar name	$S_{P_{\text{PKS}}}$ (mJy)	$S_{\text{ATCA}}$ (mJy)	$S_{\text{ATCA}}$ (mJy)
(1)	(2)	(3)	(4)
C	0.36(4)	0.24(6)	0.13
D	0.22(3)	0.37(10)	0.22
E	0.21(3)	0.08(2)	0.14
F	0.15(2)	0.18(5)	0.14
G	0.05(2)		
H	0.09(2)		
I	0.09(1)		
J	0.54(6)	0.33(9)	0.16
L	0.04(1)		
M	0.07(2)		
N	0.03(1)		
O	0.10(1)		
Q	0.05(2)		
U	0.06(1)		

- Derive the low resolution image from the modified visibility dataset, and measure the flux of all emission within  $4r_c$  of the cluster centre.
- Correct this figure for the flux scale differences between the ATCA and Parkes measurements (see section 4.2).
- Add the mean flux, as reported by Camilo et al. (2000), of each pulsar detected and subtracted in the first two analysis steps above.

## 5 RESULTS

Figure 3 shows the central part of 47 Tucanae at 20 cm before (left) and after (right) the pulsar and source removal described in section 4.5. Significant emission is visible from only a small part of the  $4r_c$  circle around the cluster centre and the total radio flux is much less than the  $\sim 4$  mJy expected if the predicted  $\sim 200$  pulsars exist in the cluster. The total flux measured in the residual image inside the  $4r_c$  circle is  $^f S_A = 0.42 \pm 0.22$  mJy. The uncertainty is calculated from the observed brightness noise in the image (0.06 mJy/beam), the error in determination of the bright pulsar flux, and an estimate of the likely difference in flux of a 48-hour integration from the long term mean flux of the weaker, un-subtracted pulsars (see section 4.3 and equation (11)). Converting the measurement to the Parkes flux scale using the factor derived in section 4.2, we have  $^f S_P = 0.52 \pm 0.28$  mJy. Thus the total 20-cm radio flux is

$$S_P = ^b S_P + ^f S_P = 2.00 \pm 0.29 \text{ mJy} \quad (12)$$

In Figure 4 we relate this result to the cumulative flux distribution. The vertical line indicates the likely lower bound to the flux of pulsars in the cluster. It is unlikely that the flux distribution extends below  $s_{\text{min}} \simeq 0.02$  mJy, corresponding to an upper bound for the pulsar population size

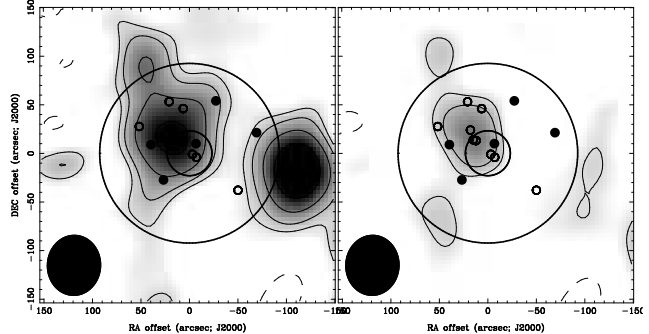


**Figure 3.** Image of the core region of 47 Tucanae. The left panel shows the radio emission from all pulsars and background sources. On the right is the residual image after subtraction of components outside the  $4r_c$  circle, pulsars C, D, E, F and J, and source S176 (see text). Image coordinates are indicated as offsets from the cluster centre:  $\alpha_{\text{J}2000} = 00:24:05.9$ ,  $\delta_{\text{J}2000} = -72:04:51.1$ . Image brightness is shown as contours at  $-2, 2, 3, 5$  &  $8 \times$  the rms fluctuation in the image of  $\sigma = 60 \mu\text{Jy}$ . The cluster core  $r_c = 23.1$  arcseconds and an area of radius  $4 \times r_c$  are indicated. The positions of the five brightest pulsars (C, D, E, F, J) are marked with  $\bullet$ . All other known pulsar positions are marked  $\circ$ . The size of the restoring beam is shown at lower left.

of  $N \lesssim 30$ . This result is consistent with the possibility that there are no further radio pulsars to be detected in 47 Tuc.

The minimum luminosity of this distribution is  $^{\text{min}} L_{1400} = s_{\text{min}} D^2 = 0.4 \text{ mJy kpc}^2$  at 1400 MHz. Pulsar luminosities are often referred to 400 MHz with a spectral index of  $-2$  assumed to allow conversion:  $L_{400} = L_{1400} (400/1400)^{-2}$ . Using this approach we estimate the lower limit of 400 MHz luminosity of the 47 Tuc pulsar population to be  $^{\text{min}} L_{400} = 6 \text{ mJy kpc}^2$ .

## 6 DISCUSSION

In this work we have estimated two parameters of the population of pulsars in 47 Tucanae: the lower bound to its luminosity distribution  $^{\text{min}} L_{1400}$  and its size  $N$ , the total number of observable pulsars in the cluster. Our technique is similar to that used by Fruchter and Goss (1990) who made measurements of integrated flux densities of a number of globular clusters and estimated the number of pulsars in each cluster. Fruchter and Goss used a luminosity function corresponding to equation 3 with an assumed value of  $^{\text{min}} L_{1400} \sim 0.2 \text{ mJy kpc}^2$ , the luminosity of the weakest millisecond pulsar known at the time of their work. In the case of 47 Tuc, we have used our measurement of the integrated flux and also the measured fluxes of the brightest members of the population to constrain both  $N$  and  $^{\text{min}} L_{1400}$ . We find  $^{\text{min}} L_{1400} \sim 0.4 \text{ mJy kpc}^2$ , significantly greater than the value assumed by Fruchter and Goss.

As we noted in the introduction, the determination of the radio luminosity distribution of pulsars is frustrated by uncertainties in pulsar distances and the difficulty of defining a sample free of strong selection effects. To make this determination usefully for all currently known millisecond pulsars is probably impossible. The pulsars in 47 Tuc provide the best opportunity available at present to characterise

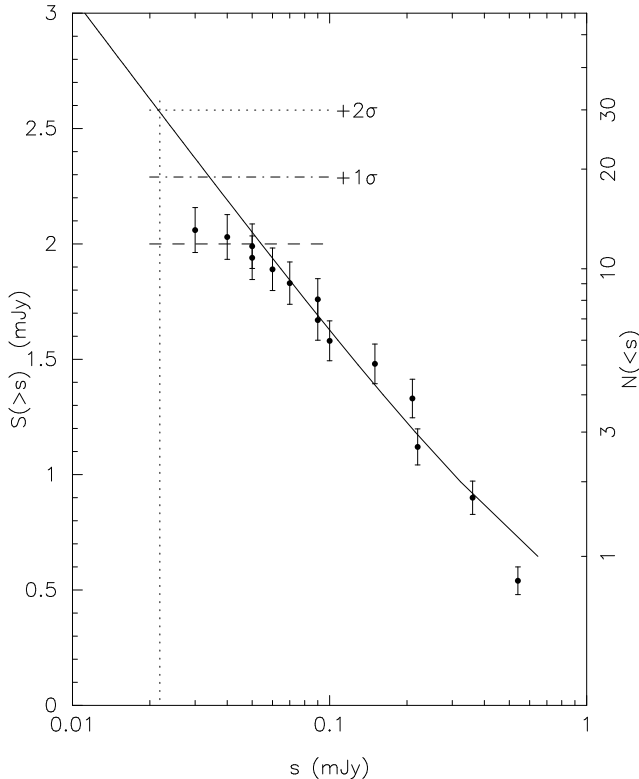


**Figure 4.** The cumulative flux distribution  $S(>s)$  of pulsars in 47 Tuc as measured by Camilo et al., 2000. The solid line shows the expected value of  $S(>s)$  corresponding to expression 7 using the fitted value of the product  $Ns_{min} = 0.66$  mJy from Figure 1. Corresponding values of the total pulsar number are shown on the right hand axis. The best estimate of total radio flux from the cluster core is indicated by the dashed line. The horizontal dotted line shows the  $2\sigma$  upper bound. The vertical dotted line indicates the likely lower bound to the pulsar flux distribution.

the radio luminosities of millisecond pulsars, and perhaps of pulsars in general.

If we accept the inferences made about the luminosity function of the 47 Tuc pulsar population, then the least luminous members of the population are nearly an order of magnitude brighter than the weakest pulsars in the general galactic population. We speculate that the origin of this difference relates more to the distinction between standard and millisecond pulsars, than to the different locations of the sample populations. The radio luminosity of an individual pulsar is expected to decline steadily, in accord with declining rotational energy. Ultimately the rotational energy reduces to the point of being insufficient to power the radio emission mechanism, and the pulsar crosses the “death line” — see for example the discussion by Chen and Ruderman (1993). As a class, the millisecond pulsars have very small values of  $\dot{P}$ , so that their evolution towards the death line is very slow. The characteristic age at which a pulsar crosses the death-line (which also corresponds to a fixed mechanical luminosity line), can be shown to be inversely proportional to its magnetic field strength. Hence, compared to normal pulsars the age at which radio millisecond pulsars die would be several orders of magnitude longer. Perhaps the relatively high low-luminosity bound inferred for the 47 Tuc pulsars

indicates how much additional time is required for them to evolve through lower luminosities to the death line.

Most energy lost from a pulsar is radiated in the form of low frequency “dipole radiation”, generated by the rotation of the star’s magnetic field and observable as the gradual increase in rotation period. A tiny fraction of the energy loss is visible in the radio spectrum. Real physical insight might be expected from successfully connecting, through measurement, the radio luminosity with the total energy loss rate. The pulsars in 47 Tuc present us with a measurable radio luminosity distribution at 1.4 GHz. Grindlay et al. (2002) estimated energy loss rates  $\dot{E}$  of the pulsars after assuming that the location of each pulsar in the cluster’s gravitational potential can be estimated from its differential dispersion measure. If the total radio luminosities could be inferred from the 1.4 GHz measurements and the likely beam solid angles, some attempt could be made to connect them to the estimates of  $\dot{E}$ .

Finally we note that X-ray detection provides an alternate means of estimating the total population of 47 Tuc. Grindlay et al. (2002) have reported *Chandra* observations and place an upper limit of 90 pulsars in the cluster. The X-rays are attributed to thermal emission from the polar cap and are not beamed. Adopting the upper limits of 90 X-ray and 30 radio pulsars, and assuming the X-rays are not beamed, the implied radio beaming factor is  $\sim 0.3$ .

In conclusion, we have determined a lower bound to the luminosity of pulsars in the globular cluster 47 Tucanae. If this bound is typical of millisecond pulsars in general, then it would imply a considerably smaller number of pulsars in globular clusters than believed earlier.

## ACKNOWLEDGEMENTS

We thank the staff of the ATCA for their expert support during this observational programme. DM is grateful for the support of the RRI during his one month study visit, during which much of this paper was written. AAD is grateful to the ATNF for support during the study visit to Australia, during which this project was initiated. We thank the referee for suggestions which led to improvements in this paper. TC was supported by an ATNF Summer Vacation scholarship. The Australia Telescope Compact Array is funded by the Commonwealth of Australia for operation as a National Facility by CSIRO.

## REFERENCES

- Alpar, M.A., Cheng, A.F., Ruderman, M.A. and Shaham, J., *Nature*, 300, 728, 1982
- Camilo, F., Lorimer, D.R., Freire, P.C., Lyne, A.G. and Manchester, R.N., *ApJ*, 535, 975, 2000
- Freire, P.C. Camilo, F., Lorimer, D.R., Lyne, A.G., Manchester, R.N. and D’Amico, N., *MNRAS*, 326, 901, 2001
- Chen, K. and Ruderman, M., *ApJ*, 402, 264, 1993
- Fruchter, A.S. and Goss, W.M., *ApJ*, 365, L63, 1990
- Howell, J.H., Guhathakurta, P. and Gilliland, R.L., *PASP*, 112, 1200, 2000
- Grindlay, J.E., Camilo, F., Heinke, C.O., Edmonds, P.D., Cohn, H., and Lugger, P., *ApJ*, 581, 470, 2002
- Lyne, A.G., Manchester, R.N., Taylor, J.H., *MNRAS*, 213, 613, 1985

McConnell, D. and Ables J.G., MNRAS, 311, 841-845, 2000  
McConnell, D., Deacon, R. and Ables, J.G., PASA, 18, 136, 2001  
Manchester, R.N., PASA, 18, 1, 2001  
Ricket, B.J., ARA&A, 15, 479, 1977  
Srinivasan, G. and van den Heuvel, E.P.J., A&A, 108, 143, 1982  
Zoccali, M. et al., ApJ, 533, 733, 2001